Rate dependency of β-adrenergic modulation of repolarizing currents in the guinea-pig ventricle

M. Rocchetti, V. Freli, V. Perego, C. Altomare, G. Mostacciuolo and A. Zaza

Dipartimento di Biotecnologie e Bioscienze, Università degli Studi Milano-Bicocca, Milano, Italy

β-Adrenergic stimulation modulates ventricular currents and sinus cycle length (CL). We investigated how changes in CL affect the current induced by isoprenaline (Iso) during the action potential (AP) of guinea-pig ventricular myocytes. Action-potential clamp was applied at CLs of 250 and 1000 ms to measure: (1) the net current induced by 0.1 μM Iso (I_{Iso}); (2) the L-type Ca^{2+} current I_{CaL} and slow delayed rectifier current I_{Ks} components of I_{Iso} (I_{IsoCa} and I_{IsoK}), identified as the Iso-induced current sensitive to nifedipine and HMR1556, respectively; and (3) I_{Iso} persisting after inhibition of both I_{Ca} and I_{Ks} (I_{isoR}). The pause dependency of I_{Ks} and its modulation were evaluated in voltage-clamp experiments. The rate dependency of the duration of the action potential at 90% repolarization (APD_{90}) and its modulation by isoprenaline were tested in current-clamp experiments. At a CL of 250 ms I_{Iso} was inward during initial repolarization and reversed at 59% of APD_{90}. At a CL of 1000 ms I_{Iso} became mostly inward in all cells. Switching to shorter CL did not change I_{IsoCa} and I_{IsoK} amplitudes, but moved their peak amplitudes to earlier repolarization; I_{IsoR} was independent of CL. Acceleration of I_{IsoK} at shorter CL was based on faster pause dependency of I_{Ks} activation rate. The 'restitution' of activation rates was modulated by isoprenaline. The APD_{90}–CL relation was rotated anti-clockwise by isoprenaline and crossed the control curve at a CL of 150 ms (400 beats min^{-1}). We conclude that: (1) isoprenaline induced markedly different current profiles according to pacing rate, involving CL-dependent I_{Ca} and I_{Ks} modulation; (2) the effect of isoprenaline on APD_{90} was CL dependent, and negligible during tachycardia; and (3) during sympathetic activation, repolarization stability may involve matched modulation of sinus rate and repolarizing currents.

(Resubmitted 9 January 2005; accepted after revision 13 February 2006; first published online 16 February 2006)
Corresponding author A. Zaza: Università di Milano-Bicocca, Dipartimento di Biotecnologie e Bioscienze, Piazza della Scienza 2, room U3-3013, 20126 Milano, Italy. Email: antonio.zaza@unimib.it

Adrenergic stimulation of ventricular muscle directly modulates membrane currents and Ca^{2+} handling. At the same time adrenergic action on the sinus node increases heart rate, which on its own has profound effects on cell electrophysiology and excitation–contraction coupling. Thus, the physiological response of the ventricle to adrenergic stimulation reflects the interplay of direct and rate-induced effects. Whether such interplay may consist of a simple summation or have a more complex nature is largely unknown.

There are diverse conditions under which adrenergic activation is not accompanied by the expected (quantitatively appropriate) increase in ventricular activation rate; they are all characterized by an abnormal susceptibility to ventricular arrhythmias, mostly attributed to repolarization abnormalities (Zlotikamien *et al.* 1990; Swan *et al.* 1999; Priori *et al.* 1999). Whilst in some conditions the mismatch between neural activity and rate response stands out as the causative abnormality (Ueda *et al.* 2004), in others it can enhance the arrhythmogenic effect of primary (Gladman *et al.* 1996) and drug-induced repolarization defects (Pinski *et al.* 2002). This leads to the hypothesis that inadequate increase in heart rate may, *per se*, change the ventricular response to adrenergic activation from normal to arrhythmogenic.

In this study we describe a remarkable rate dependency of the net membrane current induced by β-adrenergic stimulation during the ventricular action potential in guinea-pig myocytes. We also address the mechanism of such a dependency, by studying separately the contributions of the currents mostly affected by β-adrenergic stimulation (slow delayed rectifier current I_{Ks} and L-type Ca^{2+} current I_{CaL}). Focus on these currents is also justified by their time-dependent kinetics and by the importance of their balance in determining repolarization.

Methods

The present investigation conforms to the Guide to the Care and Use of Laboratory Animals published by the US

 DOI: 10.1113/jphysiol.2006.105015

National Institutes of Health (NIH publication no. 85-23, revised 1996) and to the guidelines for Animal Care endorsed by the University of Milan.

Myocyte isolation and recording apparatus

Hartley guinea-pigs (body weight ∼250 g) were killed by cervical dislocation under combined 20 mg ketamine–1.5 mg xylazine anaesthesia. Ventricular myocytes were isolated by using a retrograde coronary perfusion method previously published (Zaza *et al.* 1998), with minor modifications. Isolated myocytes were resuspended in 1 mM $CaCl_2$ Tyrode solution containing gentamycin (10 μg ml^{-1}) and stored at room temperature until use. Rod-shaped, Ca^{2+}-tolerant myocytes were used within 12 h from dissociation. Measurements were performed only in quiescent myocytes with clear-cut striations. Myocytes in suspension were placed in a 30 mm Petri dish, with a plastic ring to reduce total volume to ∼1 ml. The dish was perfused at 2 ml min^{-1} with Tyrode solution containing (mM): 154 NaCl, 4 KCl, 2 $CaCl_2$, 1 $MgCl_2$, 5 Hepes-NaOH and 5.5 D-glucose, adjusted to pH 7.35 with NaOH. The cell under study was held within 300 μm from the tip (1 mm) of a thermostated manifold pipette allowing for rapid switch between solutions (measured equilibration time < 2 s). The solution temperature was monitored at the pipette tip with a fast-response digital thermometer (BAT-12, Physitemp, Clifton, NJ, USA) and kept at $36 \pm 0.5^{\circ}$C.

Membrane potential and current measurements

Measurements were performed by the patch-clamp technique in the whole-cell configuration (Axon Multiclamp 700A, Axon Instruments). Electrodes with a tip resistance between 2.5 and 3 MΩ were pulled from borosilicate glass pipettes. The pipette solution contained (mM): 110 potassium aspartate, 23 KCl, 0.4 $CaCl_2$ (calculated free Ca^{2+} of 10^{-7} M), 3 $MgCl_2$, 5 Hepes-KOH, 1 EGTA-KOH, 0.4 GTP-Na salt, 5 ATP-Na salt, and 5 creatine phosphate Na salt, adjusted to pH 7.3 with KOH. In order to minimize impact on Ca^{2+}-dependent conductances, pipette Ca^{2+} and EGTA concentrations were selected to achieve a small residual buffering capacity (Fabiato & Fabiato, 1979), as suggested by the persistence of mechanical activity in the patched myocytes. Membrane capacitance (85.4 ± 4 pF) and series resistance (8.8 ± 0.4 MΩ) were measured in every cell ($n = 82$) according to the required compensation current (Axon Multiclamp 700A), but left uncompensated. An average junction potential of +5.5 mV, measured upon moving the electrode tip from Tyrode solution to pipette (intracellular) solution was also left uncompensated. Current signals were filtered at 2 kHz, digitized through a 12-bit A–D converter (Axon Digidata 1200; sampling rate, 5 kHz). Trace acquisition and analysis was controlled by dedicated software (Axon pClamp 8.0).

Experimental protocols

Total isoprenaline-induced current (I_{Iso}) during ventricular electrical activity was evaluated at cycle lengths (CLs) of 250 and 1000 ms by the action-potential-clamp technique (AP clamp; Doerr *et al.* 1990; Rocchetti *et al.* 2001). Isoprenaline-induced current was obtained by subtracting the current recorded in control conditions from that recorded in the presence of 0.1 μM isoprenaline.

The individual contributions of I_{CaL} and I_{Ks} modulation to I_{Iso} were evaluated by recording the currents sensitive to the selective blockers nifedipine (5 μM) and HMR1556 (1 μM; Thomas *et al.* 2003), respectively (obtained as current in control conditions minus current in the presence of the blocker). For the purpose of this analysis, results are presented as the change in each current (I_{CaL} or I_{Ks}) produced by isoprenaline, rather than the current itself. The isoprenaline-induced I_{CaL} and I_{Ks} are referred to as I_{IsoCa} and I_{IsoK}, respectively. The current induced by isoprenaline in the presence of complete I_{CaL} and I_{Ks} inhibition (I_{IsoR}) was also evaluated. Where specified, individual current and action potential traces were plotted on time scales normalized to the duration of the action potential at 90% repolarization (APD_{90}). This allowed averaging of traces obtained from different cells and favoured assessment of the contribution of each current to a specific phase of repolarization, independently of absolute APD_{90}. Nonetheless, it should be kept in mind that differences in APD_{90} are obscured by this representation. Dynamic current–voltage (I–V) relations were obtained in AP-clamp experiments by plotting membrane current traces *versus* the respective action potential waveform. Reversibility of the effects of the test solution was checked in all AP-clamp experiments, as required to rule out artifactual current changes due to time-dependent run-down. Quantification of the reversibility of the isoprenaline effect (the most prone to run-down) is provided in the online supplement (Fig. 1*S*).

Pause dependency of I_{Ks} kinetics was analysed by a traditional voltage-clamp protocol. Two activating steps (S1 and S2 to +20 mV) were separated by a pause (at −80 mV) of variable duration (Fig. 5*A*). Time-dependent I_{Ks} activation during S2 (I_{Ks} reactivation) was fitted by a single exponential to estimate the reactivation time constant (τ_{react}); the initial activation delay (about 60 ms) was not included in the fit (Tzounopoulos *et al.* 1998). Contaminating currents were minimized by adding E-4031 (5 μM, blocking the rapid delayed-rectifier current, I_{Kr}), 4-aminopyridine (3 mM, blocking the transient outward current, I_{to}), nifedipine (5 μM, blocking I_{CaL}) and nickel (5 mM, blocking I_{CaL}, the T-type Ca^{2+} current, I_{CaT} and the Na^+/Ca^{2+} exchanger current I_{NCX}) to extracellular

solutions and increasing pipette EGTA to 5 mM. The chromanol derivative HMR1556 (1 μM), a selective I_{Ks} blocker, was used to confirm that the current recorded in the modified Tyrode solution was I_{Ks} (see online supplement).

The rate dependency of APD_{90} was measured under current-clamp conditions during stimulation, delivered through the patch pipette (2 ms, amplitudes between 1.8 and 2.2 nA) at various cycle lengths (CLs, range 0.2–1.0 s). APD_{90} was measured from every beat by custom-made software. APD_{90} values were obtained from the average of at least five consecutive action potentials recorded after achievement of a steady state at each CL and after 1 min quiescence. The APD_{90}–CL relation was well fitted by the logistic type function (Zaza *et al.* 1991; Malfatto *et al.* 2003) $APD = APD_{max} \times CL^S/(CL_{50}{}^S + CL^S)$ with APD_{max} constrained at the APD_{90} value measured after prolonged (1 min) quiescence. The CL at 50% APD_{max} (CL_{50}) and slope factor (S) were estimated from the fitting.

Chemicals

HMR1556 and 9-anthracene-carboxylic acid (9-AC) were dissolved in DMSO, nifedipine in ethanol, and E-4031 in distilled water. The final DMSO or ethanol concentrations did not exceed 0.1%. HMR1556 and E-4031 were generous gifts of Aventis (Frankfurt, Germany) and Sanofi Recherche (Montpellier, France), respectively; all other chemicals were purchased from Sigma (St Louis, MO, USA).

Statistical analysis

Current magnitude was expressed as 'peak' and 'mean' values. The latter was calculated by integrating the current trace over repolarization and dividing the result by repolarization time. Current magnitudes were divided by cell capacitance to obtain current densities. Least-square fitting was used to estimate process kinetics. Student's t test or ANOVA for paired or unpaired measurements were applied as appropriate to test for significance bewteen means. *Post hoc* comparison between individual means was performed by Student's t test after Bonferroni's correction. Data are expressed and plotted as the mean ± S.E.M. value; ± S.E.M. intervals are also shown for average trace recordings. Statistical significance was defined as $P < 0.05$ (n.s., not significant). The sample size for each experiment is specified in the respective figure legend.

Results

Rate dependency of total isoprenaline-induced current (I_{Iso})

A representative example of I_{Iso} recorded at CLs of 250 and 1000 ms in the same myocyte is shown in Fig. 1*A*. Figure 1*B* shows average I_{Iso} profiles and the respective action potential waveforms obtained from all the cells tested after normalization of the time scale to APD_{90} (see Methods). During early repolarization I_{Iso} was inward, decreasing or reversing as repolarization progressed.

At a CL of 250 ms, the inward component of I_{Iso} was consistently followed by an outward one, of sizable magnitude and extending to the end of repolarization. On average, the inward component achieved a maximum in early phase 2 (time to peak, t_{peak}, at 28.5 ± 2.9% of APD_{90}), current reversal occurred at 59.3 ± 4.1% of APD_{90}, and the contribution of the outward component to total I_{Iso} was 43.5 ± 6.4%.

At a CL of 1000 ms inward I_{Iso} became strongly predominant; its amplitude increased and its peak moved to the transition between phase 2 and 3 (t_{peak} at 48.9 ± 4.8% of APD_{90}; $P < 0.05$ *versus* CL 250 ms). At this CL, the current did not reverse in three of 21 cells and in the remaining ones it became outward only at the very end of repolarization (80.1 ± 1.9% of APD_{90}); thus, on average, I_{Iso} was inward during the whole repolarization.

Diastolic I_{Iso} was inward at both CLs and larger at a CL of 250 ms (-0.77 ± 0.1 pA pF^{-1} *versus* -0.30 ± 0.07 pA pF^{-1}; $P < 0.05$).

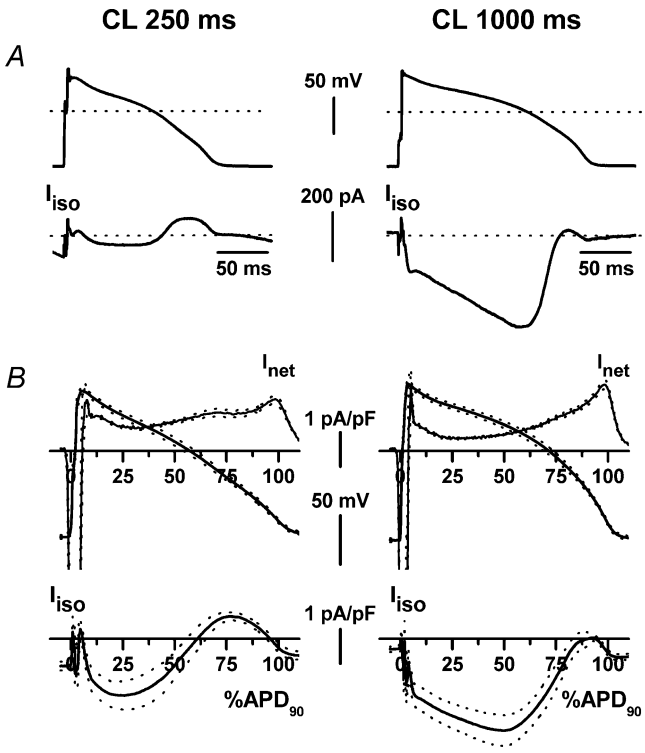

Figure 1. Cycle-length dependency of total isoprenaline-induced current (I_{Iso})
A, sample I_{Iso} recordings at the two CLs with the corresponding AP waveforms (absolute time scales). *B*, top panels show average AP waveform and net transmembrane current density ($I_{net} = -dV/dt$) required to generate it; bottom panels show I_{Iso} density. In *B* the time scale was normalized to APD_{90}. Average recordings ($n = 21$) and ± S.E.M. interval are shown by continuous and dotted lines, respectively.

I_{CaL} and I_{Ks} strongly contribute to repolarization and are well-known targets of β-adrenergic modulation (Reuter, 1983; Li *et al.* 1999; Volders *et al.* 2003). Thus, further experiments were performed to establish the individual contribution of these conductances to I_{Iso}.

Rate dependency of I_{IsoCa} (isoprenaline-induced I_{Ca})

To evaluate the contribution of calcium currents to the rate dependency of I_{Iso}, we studied modulation of the current sensitive to blockade by nifedipine. This current may include I_{CaL} plus all the other current components sensitive to changes in subsarcolemmal Ca^{2+}, including I_{Ks} (Nitta *et al.* 1994). The contribution of the latter current was evaluated in a set of preliminary experiments (not shown), in which nifedipine-sensitive current was measured with and without I_{Ks} blockade (HMR1556, 1 μM). At a CL of 250 ms HMR1556 resulted in a trend for an increase in I_{IsoCa}, thus suggesting potential Ca^{2+}-mediated enhancement of I_{Ks}. Thus, all subsequent experiments on I_{IsoCa} were performed in the presence of HMR1556 (1 μM, added to all solutions). Under such conditions I_{IsoCa} should include only the contributions of I_{CaL} and the Na^+–Ca^{2+} exchanger current (I_{NCX}).

Isoprenaline-induced I_{Ca} was obtained as the difference between nifedipine-sensitive currents recorded in the presence and absence of isoprenaline. Figure 2*A* shows a representative example of I_{IsoCa} recorded from the same myocyte at the two CLs. Average action potential waveforms and the respective I_{IsoCa} profiles obtained in a sample are shown in Fig. 2*B*. At a CL of 250 ms I_{IsoCa} consisted of a large inward current, monotonically increasing to a peak during the plateau phase of the action potential (t_{peak} at $35.6 \pm 3.9\%$ of APD_{90}). Its maximum (I_{peak}) and mean densities (I_{mean}) were 3.5 ± 0.9 and 1.76 ± 0.40 pA pF^{-1}, respectively. At a CL of 1000 ms, I_{IsoCa} activation included a slower phase leading to a delayed peak, which occurred at the transition between plateau and phase 3 repolarization (t_{peak} at $54.8 \pm 6.8\%$ of APD_{90}; $P < 0.05$ *versus* CL 250 ms). I_{peak} (3.94 ± 0.6 pA pF^{-1}) and I_{mean} (2.46 ± 0.46 pA pF^{-1}) of I_{IsoCa} densities were unchanged as compared to CL 250 ms.

Rate dependency of I_{IsoK} (isoprenaline-induced I_{Ks})

A representative example of I_{IsoK} recorded at CLs of 250 and 1000 ms in the same myocyte is shown in Fig. 3*A*. Average action potential waveforms and the respective I_{IsoK} profiles recorded in a sample are shown in Fig. 3*B*. Peak and mean I_{IsoK} densities were not significantly different between the two CLs (peak, 0.93 ± 0.2 *versus* 0.99 ± 0.2 pA pF^{-1}, n.s.; mean, 0.51 ± 0.13 *versus* 0.43 ± 0.13 pA pF^{-1}, n.s.). As shown by the average recordings in Fig. 3*B*, the instantaneous

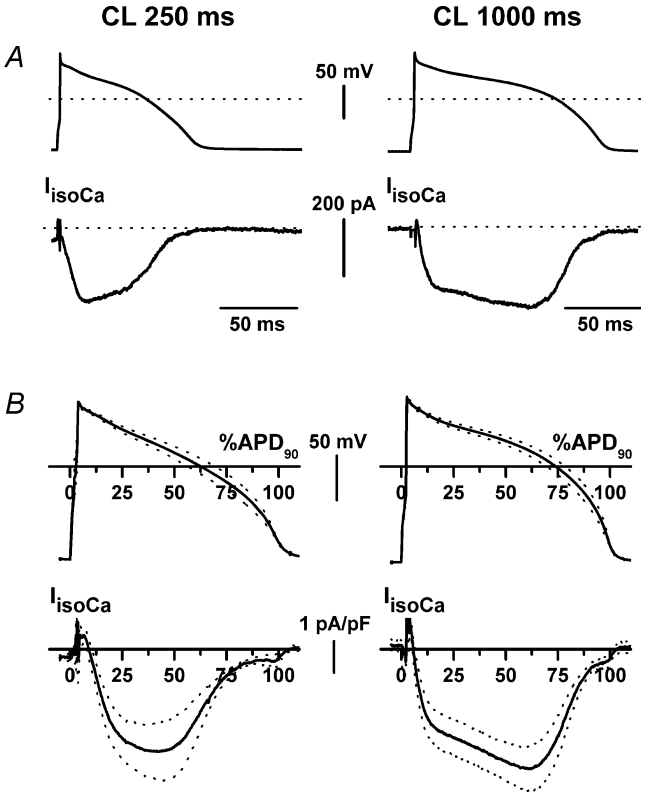

Figure 2. Cycle-length dependency of isoprenaline-induced calcium current (I_{IsoCa})
Description and symbols as in Fig. 1. For average recordings $n = 6$.

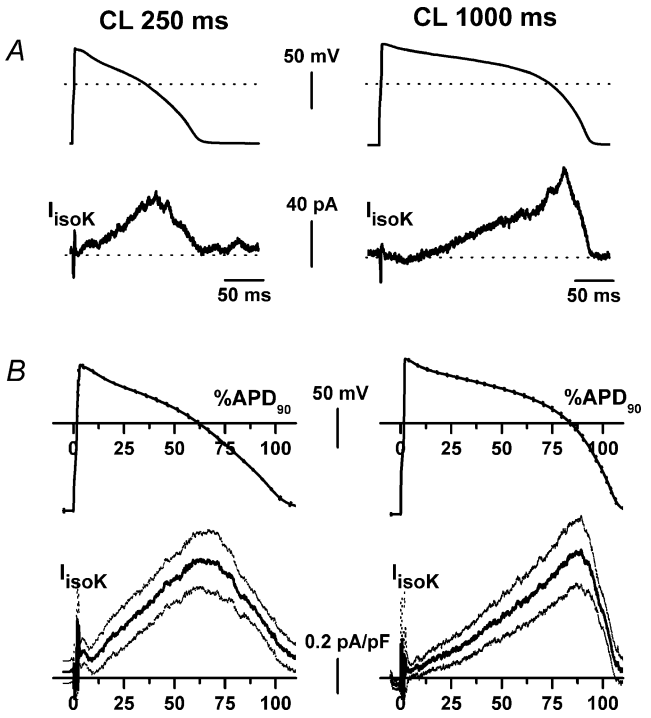

Figure 3. Cycle-length dependency of isoprenaline-induced I_{Ks} (I_{IsoK})
Description and symbols as in Fig. 1. For average recordings $n = 6$.

(time-independent) component of I_{IsoK} was almost null at a CL of 1000 ms (0.046 ± 0.050 pA pF^{-1}) and tended to increase at the shorter CL (0.187 ± 0.09 pA pF^{-1}, n.s., $n = 6$). Failure of this small change to achieve statistical significance was probably due to subtraction artifacts during the upstroke phase of individual recordings, which increased data dispersion.

At a Clof 250 ms the onset of time-dependent current was relatively fast, and I_{IsoK} achieved a maximum at 86.1 ± 11 ms (t_{peak} at $59.6 \pm 3.8\%$ of APD_{90}). At a CL of 1000 ms the onset of the time-dependent current was markedly slowed; as a consequence, peak I_{IsoK} was achieved at 205.4 ± 34.1 ms ($81.2 \pm 2.8\%$ of APD_{90}; $P < 0.05$ *versus* CL 250 ms).

To analyse the difference in the rate of I_{IsoK} onset between the two CLs independently of voltage profile, I_{Ks} conductance (G_{Ks}) profile was determined by dividing I_{Ks} by the corresponding K^+ electromotive force ($E_m - E_{Ks}$), at each instant during the action potential. E_{Ks} was -72.4 ± 1.5 mV as measured in preliminary experiments (see online supplement, Fig. 2*S*). G_{Ks} was determined at each CL in control conditions and during isoprenaline superfusion within the same myocyte. A representative example is shown in Fig. 4*A*, and the average of multiple recordings in Fig. 4*B*. The time-dependent G_{Ks} increased slightly as CL was shortened to 250 ms; this change was strongly amplified by isoprenaline, whose effect was significantly larger at a CL of 250 ms (onset rate, +356%) than at a CL of 1000 ms (onset rate, +149%; $P < 0.05$).

The mechanism of CL-dependent enhancement of I_{Ks} activation rate, observed in AP-clamp experiments, was analysed with voltage clamp by a two-step (S1–S2) protocol (see Methods). The onset of I_{Ks} was clearly composed of a time-independent (instantaneous) component and a time-dependent one (Fig. 5). As the interval between pulses was shortened, the instantaneous current during S2 increased at the expense of time-dependent current, reflecting incomplete I_{Ks} deactivation (Fig. 5*A*). At the same time, the onset of time-dependent I_{Ks} became faster, reflecting increased reactivation rate (Fig. 5*B*), a facilitation phenomenon distinct from incomplete deactivation (see Discussion). The I_{Ks} reactivation time constant (τ_{react}) increased with time from the previous pulse along an exponential 'restitution' process (Fig. 5*B*). The course of such restitution was quantified by its time constant (τ_{rest}), which was 68 ± 19 ms under control conditions. Isoprenaline slowed the restitution process (τ_{rest}, 132 ± 30 ms; $P < 0.05$ *versus* controls), thus extending facilitation of reactivation to longer interpulse intervals. Moreover, isoprenaline reduced the estimated steady-state value of τ_{react} (339 ± 8 *versus* 410 ± 9 ms; $P < 0.05$).

Residual I_{Iso} after I_{CaL} and I_{Ks} blockade (I_{IsoR})

To test for the contribution of currents other than I_{CaL} and I_{Ks} to I_{Iso} and its rate dependency, I_{Iso} was measured

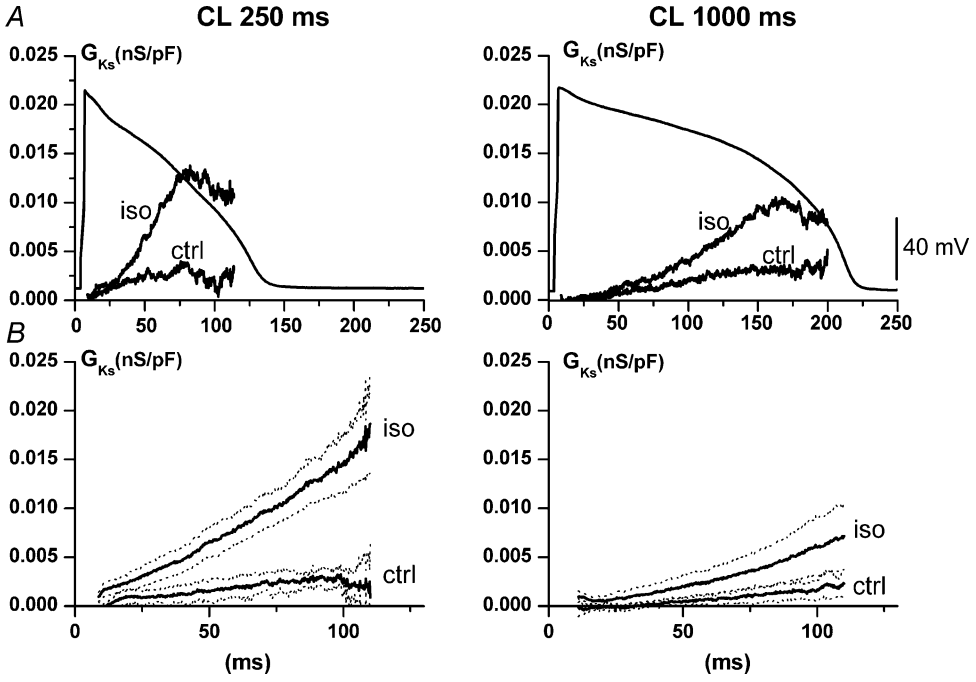

Figure 4. Cycle-length dependency of I_{Ks} conductance (G_{Ks}) and its modulation
A, representative example of G_{Ks} profile at two CLs, in control (ctrl) and during isoprenaline (Iso). *B*, average G_{Ks} profiles (continuous lines) and their ± S.E.M. interval (dotted lines; $n = 6$).

at the two CLs in the presence of 10 μM nifedipine and 1 μM HMR1556 (Fig. 6). Under such conditions isoprenaline induced a current change (residual I_{Iso}, I_{IsoR}). The I_{IsoR} profile mostly reflected the AP course, thus suggesting its origin from time-independent 'background' conductance(s) (Fig. 6*B*). The dynamic *I–V* relation (Fig. 6*C*) was linear between −60 and +40 mV. The current reversed at -31.93 ± 1.84 mV at a CL of 250 ms and at -34.9 ± 2.66 mV at a CL of 1000 ms (n.s.); the conductance (in the linear *I–V* region) was 36.1 ± 5.5 and 32.6 ± 4.5 pS pF^{-1} at CLs of 250 and 1000 ms, respectively (n.s.). Mean I_{IsoR} density was also unchanged between the two CLs (1.62 ± 0.29 *versus* 1.77 ± 0.32 pA pF^{-1}; n.s.). Minor differences in the current profiles at the two CLs reflected the different AP shapes; except for such differences, I_{Iso} measured in the absence of I_{CaL} and I_{Ks} was rate independent. The I_{IsoR} was completely and quickly reversible after isoprenaline wash out, which rules out the possibility of a leak current resulting from membrane damage. Exposure to 9-AC (100 μM), a blocker of cAMP-induced Cl^- current (Levesque *et al.* 1993) was attempted, but I_{IsoR} decrement was partial, required a long exposure time (minutes) and was irreversible. Thus, a 9-AC effect could not be safely discriminated by time-dependent current run-down. It should be stressed that 9-AC effect is generally slow in onset and decay; thus the present finding is not adequate to rule out the contribution of cAMP-induced I_{Cl} to I_{IsoR}.

Rate dependency of isoprenaline effect on action potential duration

Under control conditions APD_{90} was a saturating function of CL (Fig. 7). Within the range of CLs tested, APD_{90} was increased by isoprenaline (0.1 μM). In the presence of isoprenaline, the APD_{90}–CL relation was steeper (*S* coefficient, 2.05 ± 0.53 *versus* 1.24 ± 0.25; $P < 0.05$) and crossed the control curve at a CL of 150 ms, corresponding to a rate of 400 beats min^{-1}. Isoprenaline increased APD_{max} (226 ± 26 *versus* 184 ± 21 ms; $P < 0.05$), but not CL_{50} (208 ± 21 *versus* 199 ± 25 ms; n.s.).

Kinetics of onset of isoprenaline effects

The kinetics by which isoprenaline-induced changes occur may be relevant to the extent to which they are expressed during the continuous fluctuations peculiar to physiological neural discharge. The analysis shown in Fig. 8 addresses the CL dependency of the kinetics of isoprenaline-induced changes in APD_{90} and

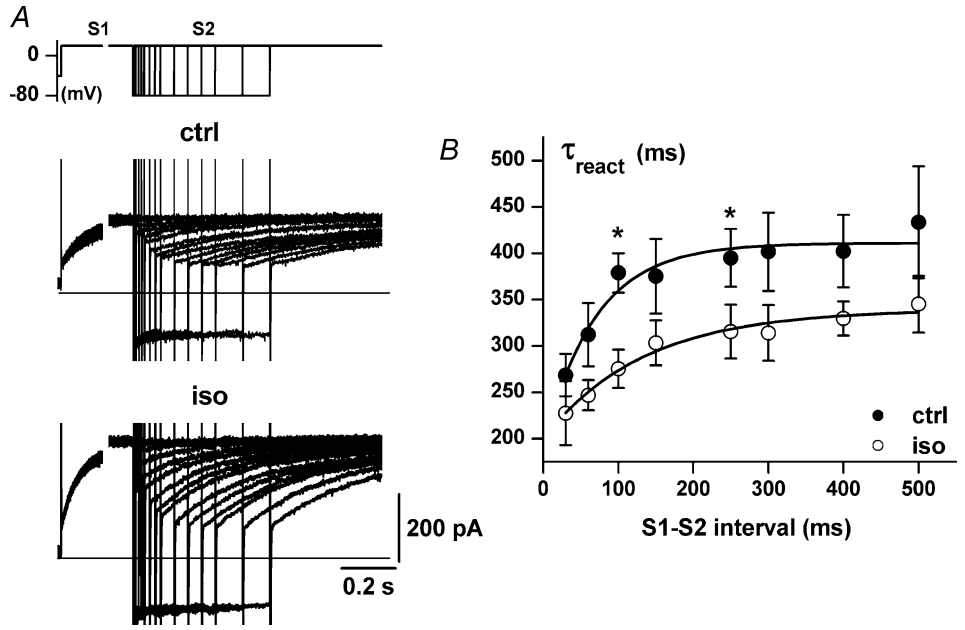

Figure 5. Pause dependency of I_{Ks} reactivation rate
A, sample recordings of I_{Ks} (protocol shown in the inset) under control conditions (ctrl) and in the presence of isoprenaline (Iso). *B*, restitution of activation kinetics. The time constant of I_{Ks} reactivation (τ_{react}), i.e. activation during S2, is plotted as a function of the S1–S2 interval. Control (●) and isoprenaline (○) data points were fitted (continuous lines) to estimate the time constant of the restitution process (τ_{rest}, see textl; $n = 5$). The overall difference between control and isoprenaline data is highly significant ($P < 0.001$ with ANOVA for repeated measurements); for individual points $^*P < 0.05$ (Bonferroni's correction).

transmembrane current. The onset of isoprenaline effects was characterized by an initial lag, followed by a time course well fitted by an exponential function. For both APD_{90} (current clamp, Fig. 8*A*) and transmembrane current (AP clamp, Fig. 8*B*), the rate of onset increased as CL was shortened. The exponential time constants (τ) for APD_{90} and membrane current were comparable and changed similarly as a function of CL (Fig. 8*C*). The CL dependency of τ was steeper at short CLs (τ doubled between 250 and 500 ms), showing saturation at longer CLs.

Discussion

Interpretation of action-potential-clamp experiments

Any difference in net membrane current caused by receptor stimulation (primary effect) changes the action potential profile. Since most of cardiac channels are voltage gated, the change in voltage feeds back on currents, causing further changes (secondary effects). Such a loop eventually leads to a stable action potential profile, usually identified as the consequence of the intervention, which is possibly different from that resulting from the primary effect. The action-potential-clamp technique aims to identify the primary effect of receptor stimulation by interrupting the current–voltage interaction loop. At variance with traditional (square-wave) voltage-clamp experiments, the primary effect is analysed in the context of physiological voltage profiles and repetitive activity. While unsuited to the assessment of channel gating properties, this approach highlights features of the response to an intervention that may otherwise remain concealed.

Changes in diastolic interval as well as in action potential shape can contribute to the rate dependency of ionic conductances during phyisiological activity (Rocchetti *et al.* 2001). Action potential templates specific for each CL were used in the present experiments; thus, rate dependency included both the factors mentioned above, and no attempt was made to discriminate between them.

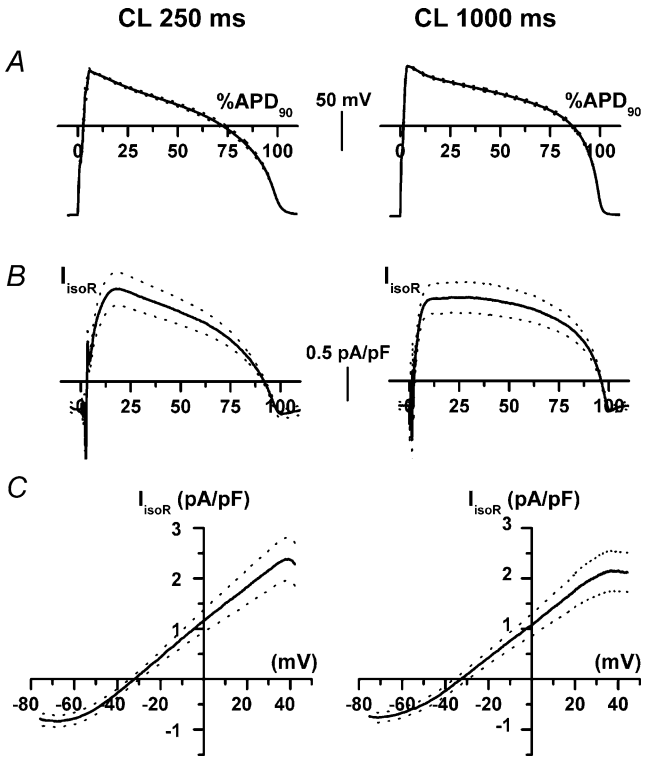

Figure 6. Cycle-length dependency of I_{Iso} after I_{CaL} and I_{Ks} blockade (I_{IsoR})
A, average action potential waveforms. *B*, average I_{IsoR} density recorded at the two CLs during the action potentials shown in *A* (time scales normalized to APD_{90}). *C*, average dynamic *I–V* relations of I_{IsoR}. Average recordings ($n = 12$) and their ± S.E.M. limits are shown by continuous and dotted lines, respectively.

Rate dependency of I_{Iso} during ventricular action potential

Total isoprenaline-induced current (I_{Iso}) recapitulates all current changes directly or indirectly induced by β-receptor stimulation and represents the primary drive for the agonist-induced changes in the action potential contour. I_{Iso} includes channels of different selectivity, variably activated during the action potential course; this accounts for the biphasic profile of I_{Iso}. Such a profile

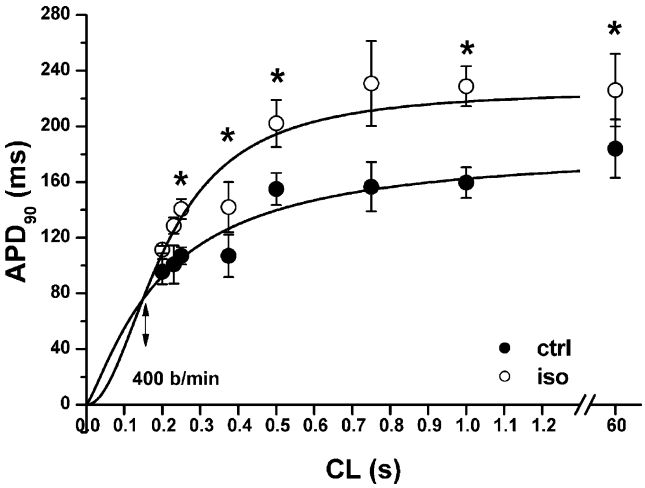

Figure 7. Cycle-length dependency of APD_{90} and its modulation
APD_{90} measured during steady-state pacing at various CLs under control conditions (●) and in the presence of isoprenaline (○; $n = 3$ at all CLs). The continuous lines are logistic data fits, for which the asymptote was fixed at the 60 s APD_{90} value. The double-headed arrow indicates the heart rate at which the extrapolated APD_{90}–CL relations cross (i.e. APD_{90} would be unaffected by isoprenaline). The overall difference between control and isoprenaline data is highly significant ($P < 0.001$ with ANOVA); for individual data points $^*P < 0.05$ (Bonferroni's correction).

was profoundly affected by stimulation rate, with changes in the inward:outward current ratio and in the timing of each component with respect to repolarization phase. Timing changes may be relevant because they strongly affect the voltage response to current flow. In particular, the transition between plateau and terminal repolarization is a critical phase because of its proximity to the threshold of autoregenerative phenomena leading either to full repolarization (I_{Kr} or I_{K1}, the inward-rectifier current) (Rocchetti *et al.* 2001; Biliczki *et al.* 2002) or to abnormal depolarization (I_{CaL}; January & Riddle, 1989; Zeng & Rudy, 1995), depending on net current balance. During this phase I_{Iso} was null or outward at short CL and strongly inward at long CL. This suggests that the safety margin for terminal repolarization (also named 'repolarization reserve'; Biliczki *et al.* 2002) may be preserved during sympathetic activation only in the presence of an 'appropriate' increase in ventricular rate. In other words, robust repolarization may require a match between the responses of heart rate and ventricular currents to adrenergic activation. According to this interpretation, any mismatch condition (e.g. limiting the increase in ventricular rate) would alter repolarization reserve.

Rate dependency of I_{Iso} is reflected in rate dependency of APD_{90} modulation. Indeed, while APD_{90} was markedly prolonged by isoprenaline at long CLs, the fitted APD_{90}–CL relations predicted that minimal APD_{90} change would occur at rates (400 beats min^{-1}) compatible with adrenergically induced tachycardia in guinea-pigs (Hamlin *et al.* 2003). Although at long CL the I_{Iso} profile was suitable to facilitate early after-depolarizations, such phenomena seldom occurred under current-clamp conditions. This suggests that in the guinea-pig secondary current changes, occurring under current-clamp conditions, could still buffer the primary effect of β-receptor stimulation (seen under AP-clamp conditions), irrespective of stimulation rate. However, larger mammals are notoriously less resistant to repolarization abnormalities than guinea-pigs, possibly owing to differences in I_{Ks} expression (Biliczki *et al.* 2002); thus, their repolarization might be more sensitive to combined adrenergic activation and low rate.

The time course of I_{Iso} and APD_{90} changes during isoprenaline challenge displayed remarkable CL dependency. Since isoprenaline effects were slower than solution equilibration time (see Methods), their course is conceivably inherent to the biological response, whose mechanism may deserve further investigation. Faster onset implies that a larger proportion of steady-state effect will be effectively expressed during

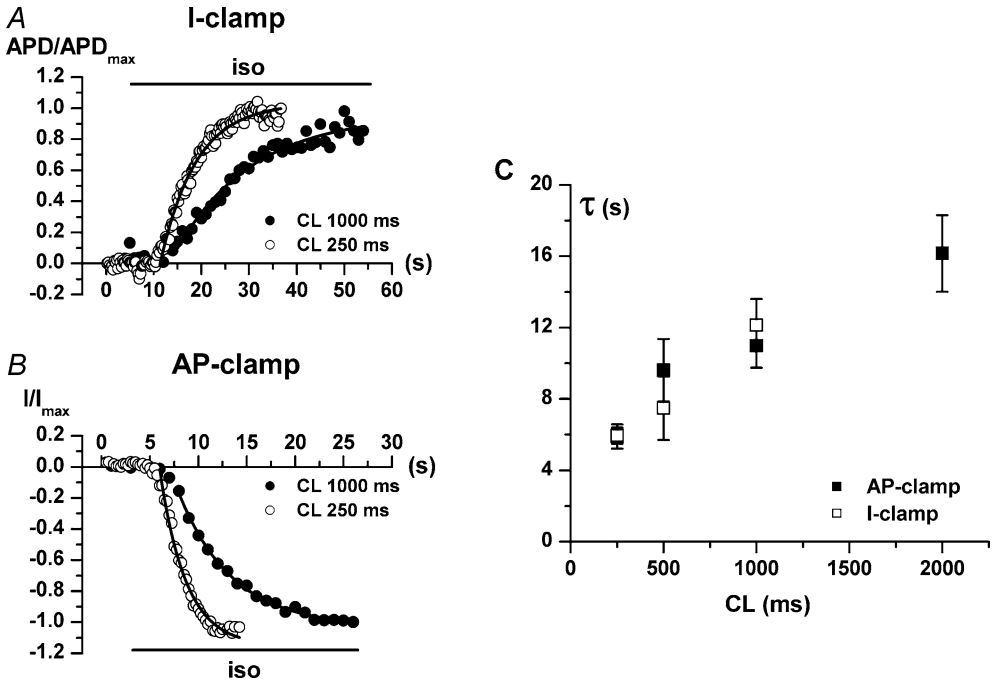

Figure 8. Rate of onset of isoprenaline effects on APD_{90} and membrane current
The time of occurrence of peak inward I_{Iso} (at steady-state isoprenaline superfusion) was used in each cell as the reference point for current measurement. *A* and *B* show examples of the time course of the APD_{90} (current clamp) and membrane current (AP clamp) responses to isoprenaline (horizontal bar). To highlight CL-dependent changes in the kinetics of response, APD_{90} (APD) and current (*I*) were normalized to the steady-state value achieved at each CL (APD_{max} and I_{max}, respectively). Continuous lines represent fitting of the exponential phase of response. *C*, time constants (τ) of APD_{90} (□, $n \geq 8$ at each CL) and membrane current (■, $n \geq 7$ at each CL) response as a function of CL.

a rise in sympathetic activity, thus resulting in more efficient adaptation of repolarization at shorter CL. This emphasizes again the interplay between the response of ventricular currents and pacemaker activity in adrenergic modulation of repolarization. APD_{90} and membrane current were measured in separate groups of cells by different experimental approaches (current clamp *versus* AP clamp). The close similarity in the time course of their response suggests that I_{Iso} adequately describes primary modulation of repolarization by β-receptors.

Rate dependency of I_{Iso} components

Rate-dependent changes in I_{IsoCa} and I_{IsoK} mostly consisted of a shift in current distribution during repolarization. Indeed, neither mean nor peak current values varied significantly between the two CLs (but see section on Limitations of the study).

At short CL I_{IsoCa} onset was monotonic and fast; a peak was achieved in the early plateau phase (36% of APD_{90}). An increase in inward current with this timing may not jeopardize repolarization because the resulting positive shift in membrane potential would accelerate I_{Ks} activation; this, in turn, would balance the excess inward current. Moreover, at this time, I_{CaL} may still be largely inactivated and unavailable for reactivation. At the longer CL I_{IsoCa} continued to rise during the plateau phase, to peak in the proximity of the transition to final repolarization. As previously mentioned, this is a critical phase because I_{CaL} may have partly recovered from inactivation and may enter an autoregenerative reactivation loop with membrane potential (January *et al.* 1988; January & Riddle, 1989). If this occurs, repolarization may be interrupted by early afterdepolarizations.

At shorter CL the instantaneous component of I_{IsoK} showed a tendency to increase, but the most dramatic change was acceleration of the onset of the time-dependent component. This caused a shift in the distribution of I_{IsoK} to an earlier phase of the action potential. Two mechanisms may contribute to rate-dependent changes in membrane current: (1) changes in the driving force, due to differences in the action potential contour and/or in the equilibrium potential of the permeant ion; and (2) changes in channel conductance, mainly due to the complex interplay between time-dependent gating and membrane potential time course. In the case of I_{IsoCa}, discrimination between these mechanisms is difficult because the profile of intracellular Ca^{2+} transients is affected by both rate and β-receptor activation, thus making any estimate of Ca^{2+} driving force impossible. In contrast, in isolated myocytes K^+ equilibrium potential can be assumed to be constant throughout the cycle; thus, the mechanism of the rate dependency of I_{Ks} and its adrenergic modulation could be investigated in more detail. The data presented in Fig. 4 clearly show that I_{IsoK} acceleration at shorter CLs is caused by a conductance change, rather than simply reflecting a different voltage profile.

A potential contribution of cytosolic Ca^{2+} to I_{Ks} rate dependency was suggested by the observed trend in I_{IsoCa} enhancement by HMR1556. However, CL dependency of I_{Ks} was mainly determined by the kinetics of channel gating. This is currently attributed to slow diastolic deactivation of I_{Ks}, which would lead to 'accumulation' of channels in the open state preferentially at short CLs (Zeng & Rudy, 1995; Stengl *et al.* 2003; Terrenoire *et al.* 2005). However, such a mechanism could account for the CL-dependent increase in the instantaneous component of G_{Ks}, but not for acceleration of the time-dependent one. Indeed, the latter component implies a faster transition from close to open states, i.e. a change in channel activation kinetics (Silva & Rudy, 2005). To address this issue, isoprenaline modulation of I_{Ks} gating was analysed by a square-wave voltage-clamp protocol, under conditions ruling out the contribution of changes in cytosolic Ca^{2+} (both I_{CaL} and I_{NCX} blocked). Such experiments showed that I_{Ks} activation rate depends on the pause between two activations. Activation rate undergoes a restitution process with smaller time constants occurring at shorter pauses. The restitution process was slowed by isoprenaline, thus enhancing the range of diastolic intervals over which activation rate is CL dependent. A similar restitution of activation kinetics was reported for channels resulting from KCNE1 protein transfection in oocytes endogenously expressing KVLQT1 protein (Tzounopoulos *et al.* 1998). This observation was interpreted as a voltage-dependent transition between two sets of channel states, with different kinetics of the opening reaction. The present data extend this observation to native I_{Ks} and show that this process is modulated by β-adrenergic stimulation. The rate-dependent G_{Ks} increase observed in the present study under control conditions was smaller than that previously reported (Rocchetti *et al.* 2001). This quantitative discrepancy may reflect small differences in diastolic potential on which deactivation rate steeply depends.

After I_{CaL} and I_{Ks} inhibition, isoprenaline activated a background current compatible with cAMP-induced I_{Cl}, though not obviously sensitive to 9-AC. It should be stressed that I_{IsoR} might be a composite current and that the conditions under which I_{IsoR} was measured are likely to affect the intracellular milieu. Thus, there is no guarantee that I_{IsoR} is carried by an individual channel, or that it contributes to total I_{Iso} in its full extent; nonetheless, the sum $I_{IsoCa} + I_{IsoK} + I_{IsoR}$ roughly matched total I_{Iso} in terms of magnitude and dependency on CL (see online supplement, Fig. 5*S*). The I_{IsoR} conductance was CL independent. At a CL of 250 ms, I_{IsoR} driving force during late repolarization was reduced due to steeper action potential phase 2; thus, I_{IsoR} cannot account for the increase in outward I_{Iso} observed at shorter CL.

Implications

The rate dependency of I_{Iso} distribution suggests that ventricular repolarization reserve might be reduced in all conditions characterized by a mismatch between increased sympathetic drive and heart rate response. Among the many lines of evidence in support of this view, two are particularly suggestive. The first one is the experimental observation that, after selective ablation of sympathetic nerves directed to the sinus node (right stellectomy), cats exposed to psychological stress developed repolarization abnormalities and arrhythmias (Schwartz *et al.* 1991). The second is a recent report of QT prolongation, 'torsade de pointes' ventricular tachycardia (TdP) and syncope upon sudden auditory stimuli in a patient with severe sinus node dysfunction caused by deficiency of the pacemaker current I_f (HCN4 mutation; Ueda *et al.* 2004). Notably, neither direct causes of repolarization abnormality nor signs of cardiomyopathy were found in this patient (Prof. A. Kimura, personal communication). These are extreme examples, in which arrhythmias were associated with severe bradycardia; nonetheless, milder mismatch between sympathetic drive and heart rate might reduce repolarization reserve and facilitate induction of TdP by other causes. This leads to the view that the extent of sinus rate response to sympathetic activation might be a factor in determining the widely variable penetrance and prognosis of congenital and drug-induced repolarization abnormalities (Priori, 2004; Shimizu *et al.* 2004). The practical implications of this view include reinforced indications to rate responsive pacing and restrictions in the use of 'pure bradycardic agents' (I_f blockers) in individuals exposed to risk of repolarization abnormality.

Limitations of the study

In action-potential-clamp experiments, individual currents were identified as being blocker-sensitive; thus, their magnitude and profile depend on the selectivity and potency of the blocker used. Experimental results and a detailed discussion on the methods used for current dissection in AP-clamp experiments are provided in the online supplement (Figs 3*S* and 4*S*).

Some intracellular Ca^{2+} buffering was required in all experiments; thus, the influence of cytosolic Ca^{2+} on membrane conductances might be underestimated. To minimize this potential artifact, buffering was limited to a minimum (see Methods) and was still compatible with cell contraction.

Recent reports suggest that the role of I_{Ks} in rate adaptation of APD_{90} may be larger in guinea-pigs than in larger mammals (Volders *et al.* 2003; Zicha *et al.* 2003), including man (Virag *et al.* 2001). This conclusion was based on the smaller magnitude and faster I_{Ks} deactivation found in larger mammals, which minimizes rate-dependent accumulation of the instantaneous I_{Ks} component (Stengl *et al.* 2003). According to this view, the value of the present findings would be limited by its species specificity. In contrast, also in the present experiments, changes in the instantaneous component contributed minimally to the rate dependency of I_{Ks} conductance (see Figs 3 and 4). Thus, also in the guinea-pig, incomplete diastolic deactivation may play a minor role. The major contribution to rate dependency of I_{Ks} was indeed based on acceleration of the time-dependent component, whose role can be readily appreciated only when the action potential waveform is used to drive membrane potential, as in the present experiments. Repolarization abnormalities resulting from I_{Ks} deficiency (Roden *et al.* 1996) suggest that, even if scantily expressed in isolated human myocytes, this current plays a functional role also in humans.

This study addresses the effect of β-adrenergic stimulation, which prevails in the modulation of repolarizing currents. Nonetheless, these currents may also be affected by α-receptors, which would also contribute under physiological conditions.

References

Biliczki P, Virag L, Iost N, Papp JG & Varro A (2002). Interaction of different potassium channels in cardiac repolarization in dog ventricular preparations: role of repolarization reserve. *Br J Pharmacol* **137**, 361–368.

Doerr T, Denger R, Doerr A & Trautwein W (1990). Ionic currents contributing to the action potential in single ventricular myocytes of the guinea pig studied with action potential clamp. *Pflugers Arch* **416**, 230–237.

Fabiato A & Fabiato F (1979). Calculator programs for computing the composition of the solutions containing multiple metals and ligands used for experiments in skinned muscle cells. *J Physiol (Paris)* **75**, 463–505.

Gladman G, Davis AM, Fogelman R, Hamilton RM & Gow RM (1996). Torsade de pointes, acquired complete heart block and inappropriately long QT in childhood. *Can J Cardiol* **12**, 683–685.

Hamlin RL, Kijtawornrat A, Keene BW & Hamlin DM (2003). QT and RR intervals in conscious and anesthetized guinea pigs with highly varying RR intervals and given QTc-lengthening test articles. *Toxicol Sci* **76**, 437–442.

January CT & Riddle JM (1989). Early afterdepolarizations: mechanism of induction and block. A role for L-type Ca^{2+} current. *Circ Res* **64**, 977–990.

January CT, Riddle JM & Salata JJ (1988). A model for early afterdepolarizations: induction with the Ca^{++} channel agonist Bay K 8644. *Circ Res* **62**, 563–571.

Levesque PC, Clark CD, Zakarov SI, Rosenshtraukh LV & Hume JR (1993). Anion and cation modulation of the guinea-pig ventricular action potential during beta-adrenoceptor stimulation. *Pflugers Arch* **424**, 54–62.

Li GR, Yang B, Feng J, Bosch RF, Carrier M & Nattel S (1999). Transmembrane I_{Ca} contributes to rate-dependent changes of action potentials in human ventricular myocytes. *Am J Physiol* **276**, H98–H106.

Malfatto G, Facchini M & Zaza A (2003). Characterization of the non-linear rate-dependency of QT interval in humans. *Europace* **5**, 163–170.

Nitta J-I, Furukawa T, Marumo F, Sawanobori T & Hiraoka M (1994). Subcellular mechanism for Ca^{2+}-dependent enhancement of delayed rectifier K^+ current in isolated membrane patches of guinea pig ventricular myocytes. *Circ Res* **74**, 96–104.

Pinski SL, Eguia LE & Trohman RG (2002). What is the minimal pacing rate that prevents torsades de pointes? Insights from patients with permanent pacemakers. *Pacing Clin Electrophysiol* **25**, 1612–1615.

Priori SG (2004). Inherited arrhythmogenic diseases: the complexity beyond monogenic disorders. *Circ Res* **94**, 140–145.

Priori SG, Barhanin J, Hauer RW, Haverkamp W, Jongsma HJ, Kleber AG *et al*. (1999). Genetic and molecular basis of cardiac arrhythmias – Impact on clinical management. *Eur Heart J* **20**, 174–195.

Reuter H (1983). Calcium channel modulation by neurotransmitters, enzymes and drugs. *Nature* **301**, 569–574.

Rocchetti M, Besana A, Gurrola GB, Possani LD & Zaza A (2001). Rate dependency of delayed rectifier currents during the guinea-pig ventricular action potential. *J Physiol* **534**, 721–732.

Roden DM, Lazzara R, Rosen M, Schwartz PJ, Towbin J & Vincent GM (1996). Multiple mechanisms in the long-QT syndrome. Current knowledge, gaps, and future directions. The SADS Foundation Task Force on LQTS. *Circulation* **94**, 1996–2012.

Schwartz PJ, Zaza A, Locati E & Moss AJ (1991). Stress and sudden death. The case of the long QT syndrome. *Circulation* **83** (Suppl. II), 71–80.

Shimizu W, Horie M, Ohno S, Takenaka K, Yamaguchi M, Shimizu M *et al*. (2004). Mutation site-specific differences in arrhythmic risk and sensitivity to sympathetic stimulation in the LQT1 form of congenital long QT syndrome: multicenter study in Japan. *J Am Coll Cardiol* **44**, 117–125.

Silva J & Rudy Y (2005). Subunit interaction determines I_{Ks} participation in cardiac repolarization and repolarization reserve. *Circulation* **112**, 1384–1391.

Stengl M, Volders PG, Thomsen MB, Spatjens RL, Sipido KR & Vos MA (2003). Accumulation of slowly activating delayed rectifier potassium current (I_{Ks}) in canine ventricular myocytes. *J Physiol* **551**, 777–786.

Swan H, Viitasalo M, Piippo K, Laitinen P, Kontula K & Toivonen L (1999). Sinus node function and ventricular repolarization during exercise stress test in long QT syndrome patients with KvLQT1 and HERG potassium channel defects. *J Am Coll Cardiol* **34**, 823–829.

Terrenoire C, Clancy CE, Cormier JW, Sampson KJ & Kass RS (2005). Autonomic control of cardiac action potentials: role of potassium channel kinetics in response to sympathetic stimulation. *Circ Res* **96**, e25–e34.

Thomas GP, Gerlach U & Antzelevitch C (2003). HMR 1556, a potent and selective blocker of slowly activating delayed rectifier potassium current. *J Cardiovasc Pharmacol* **41**, 140–147.

Tzounopoulos T, Maylie J & Adelman JP (1998). Gating of I_{sK} channels expressed in *Xenopus* oocytes. *Biophys J* **74**, 2299–2305.

Ueda K, Nakamura K, Hayashi T, Inagaki N, Takahashi M, Arimura T *et al*. (2004). Functional characterization of a trafficking-defective HCN4 mutation, D553N, associated with cardiac arrhythmia. *J Biol Chem* **279**, 27194–27198.

Virag L, Iost N, Opincariu M, Szolnoky J, Szecsi J, Bogats G *et al*. (2001). The slow component of the delayed rectifier potassium current in undiseased human ventricular myocytes. *Cardiovasc Res* **49**, 790–797.

Volders PG, Stengl M, van Opstal JM, Gerlach U, Spatjens RL, Beekman JD *et al*. (2003). Probing the contribution of I_{Ks} to canine ventricular repolarization: key role for β-adrenergic receptor stimulation. *Circulation* **107**, 2753–2760.

Zaza A, Malfatto G & Schwartz PJ (1991). Sympathetic modulation of the relation between ventricular repolarization and cycle length. *Circ Res* **68**, 1191–1203.

Zaza A, Rocchetti M, Brioschi A, Cantadori A & Ferroni A (1998). Dynamic Ca^{2+}-induced inward rectification of K^+ current during the ventricular action potential. *Circ Res* **82**, 947–956.

Zeng J & Rudy Y (1995). Early afterdepolarizations in cardiac myocytes: mechanism and rate dependence. *Biophys J* **68**, 949–964.

Zicha S, Moss I, Allen B, Varro A, Papp J, Dumaine R *et al*. (2003). Molecular basis of species-specific expression of repolarizing K^+ currents in the heart. *Am J Physiol Heart Circ Physiol* **285**, H1641–H1649.

Zlotikamien B, Kusniec J, Strasberg B, Erdman S, Sclarovsky S & Agmon J (1990). Torsades de Pointes as a complication of bradyarrhythmias. *Isr J Med Sci* **26**, 102–105.

Acknowledgements

We are grateful to Professors A. Kimura (Medical and Dental University, Tokyo, Japan) and P. J. Schwartz (Department of Cardiology, University of Pavia, Italy) for providing information and insightful criticism to the manuscript and to Dr N. Szentandrassy (University of Debrecen, Hungary) for participating in some of the experiments. This work was partly funded by the Italian–Hungarian Cooperation program of the Italian Ministry of Foreign Affairs (to A. Zaza).

Supplemental material

The online version of this paper can be accessed at:
DOI: 10.1113/jphysiol.2006.105015
http://jp.physoc.org/cgi/content/full/jphysiol.2006.105015/DC1
and contains supplemental material concerning 1) reversibility and specifity of current block used in AP-clamp experiments, 2) comparison between I_{Iso} and the sum of its individual components (I_{IsoCa} + I_{IsoK} + I_{IsoR}), 3) experimental determination of the reversal potential of I_{Ka}.

This material can also be found as part of the full-text HTML version available from http://www.blackwell-synergy.com